Sliding Mode Based Position and Attitude Controller for a Vectored Thrust Aerial Vehicle

Hiranya Jayakody and Jay Katupitiya
School of Mechanical and Manufacturing Engineering,
University of New South Wales, Sydney, Australia
{hiranya.jayakody@student.unsw,j.katupitiya@unsw,}.edu.au

Abstract

This paper presents robust control of a Vectored Thrust Aerial Vehicle (VTAV) based on Sliding Mode Control (SMC) methodology. The VTAV is designed to be able to translate with zero roll and pitch angles so that a set of sensor suite can effectively be used for terrain mapping. Furthermore, The three thrust inputs and two thrust vectoring inputs provide more maneuverability compared to the popular quadrotor platform. First the non-linear dynamic model of the VTAV is presented. Then, contrary to existing work, the nonlinear dynamic model of the VTAV is used without any linearization process to implement a Sliding Mode based controller by introducing a set of virtual control inputs which effectively decouples the nonlinear dynamic equations of the VTAV. By solving the virtual inputs simultaneously, the real control inputs are found. Simulation results are presented to demonstrate the successful operation of the designed control system.

Keywords: Vectored thrust aerial vehicles, Sliding mode control, Nonlinear dynamic model, Zero roll pitch flight, Unmanned Aerial Vehicle

1 Introduction

Autonomous Control of Unmanned Aerial Vehicles (UAV) has become a topic of growing interest among researchers owing to their wide range of civil and military applications. Unmanned Miniature Aerial Vehicles are currently used in applications such as surveillance, traffic monitoring, object tracking and entertainment industry as well as various other military applications [Naldi *et al.*, 2010][Bertrand *et al.*, 2011]. The Vertical Take Off and Landing (VTOL) capability of UAVs has further enhanced their use in congested environment where the UAV has limited space for take-off and landing [Johnson and Turbe, 2006][Pflimlin *et al.*, 2010].

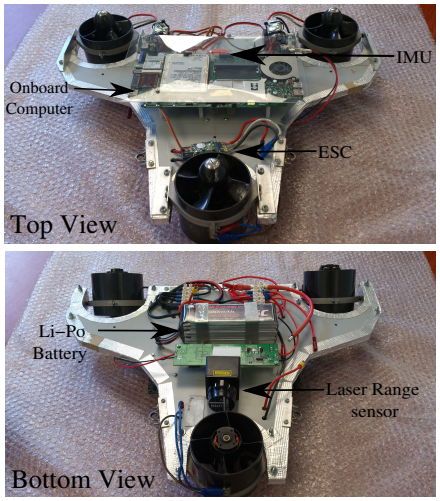

Figure 1: The Vectored Thrust Aerial Vehicle (VTAV)

Since the introduction of the Hiller platform VZ-1 in 1950s [Pflimlin *et al.*, 2010], there have been various platforms of ducted fan UAVs, each having its own pros and cons depending on the number of ducted fans, number of control inputs, physical layout etc. In contrast to those UAV designs, the work presented in this paper focuses on a novel platform with ducted fan vectoring capability, as the test bed [Kumon *et al.*, 2010][Yuan *et al.*, 2012][Yuan and Katupitiya, 2013] for the proposed controller .

The UAV design used in this paper - the Vectored Thrust Aerial Vehicle (VTAV) - consists of three ducted fans as shown in Figure 1. The rear two ducted fans can be vectored around an axis common to both ducted fans-the axis S_2S_3- as illustrated in Figure 2. The vectoring capability of this vehicle not only allows it to translate in space with minimal roll and pitch, but also increases the number of available control inputs which enhances the resilience against external disturbances. However, this vectoring capability itself leads to complex nonlinear vehicle dynamics which require sophisticated control methodologies for autonomous operation.

Both linear and nonlinear control methodologies

have been proposed for different UAV platforms with the aim of implementing robust, reliable autopilots with fast maneuverability [Zhang *et al.*, 2010][Naldi *et al.*, 2008][Yu *et al.*, 2010][Wang *et al.*, 2007]. However, compared to nonlinear controllers, linear controllers based on the linearized hover models have limited capability of stabilizing the plant when subjected to unpredictable disturbances in the environment such as wind gusts, dynamic coupling of states/inputs and model uncertainties [Derafa *et al.*, 2012]. Hence, such controllers are limited to operations around the hover condition. These limitations call for robust nonlinear control methodologies where the model uncertainties and system disturbances do not affect the operation of the controller adversely.

The Sliding Mode Control (SMC) methodology has proved to be a promising robust and reliable control method which is applicable to systems with uncertainties and external disturbances [Utkin, 1977][Slotine and Li, 1991]. The SMC methodology is capable of driving the states of a given plant to reach a set of predefined sliding manifolds within a finite time, ensuring that the system is insensitive to parametric uncertainties and external disturbances during the convergence phase. This fact has recently motivated researchers to apply SMCs in the area of UAVs for the following reasons.

- Dynamic equations of the UAVs are often nonlinear and complex, and may contain parametric uncertainties and unmodelled dynamics.
- External disturbances such as sudden wind gusts affect the operation of UAV systems adversely and therefore the controller developed must be robust to such conditions.

The applicability of SMC on UAVs is explored in [Derafa *et al.*, 2012],[Hess and Wells, 2003],[Hess and Bakhtiari-Nejad, 2008],[Khelfi and Kacimi, 2012] and [Guruganesh *et al.*, 2012]. In [Derafa *et al.*, 2012] and [Hess and Wells, 2003] a SMC based approach was followed to develop an attitude stabilizer for the UAV, which assists the human pilot. In [Khelfi and Kacimi, 2012] and [Guruganesh *et al.*, 2012] SMC based attitude and position controllers were developed for quadrotors. In most of the literature, the UAV system under consideration is linearized under different conditions with the aim of simplifying the control design through direct state-space approaches.

Considering all these facts the aim of this paper is to directly utilize the nonlinear dynamics of the VTAV in implementing a Sliding Mode based controller. The main contributions of this paper can be identified as follows.

- Developing a nonlinear robust controller which has the ability to control the VTAV over a wider range of operating conditions, in contrast to [Kumon *et al.*, 2010] and [Yuan and Katupitiya, 2013] in the presence of external disturbances and model uncertainties.
- One of the main advantages of the VTAV is its ability to fly with zero roll and pitch. However, the vehicle is underactuated in the lateral, y_b, direction (see Figure 2). In order to avoid undesirable drift in y_b direction due to wind gusts, a control topology is proposed such that the vehicle creates a non zero roll motion to avoid such drifts, *only* when wind gusts are present in y_b direction.
- A detailed analysis of the vehicle performance under the effects of wind gusts, parametric uncertainties and unmodelled dynamics is presented in order to exemplify the robust nature of the controller.

The work presented in this paper is the first implementation of a nonlinear control methodology on the VTAV. Furthermore, the boundary layer approach is utilized to avoid chattering caused by excitation of actuator dynamics [Utkin *et al.*, 2009]. Simulations carried out show that the proposed controller performs well under external disturbances and parametric uncertainties.

The paper is organized as follows. In Section 2 the dynamic model of the VTAV is derived based on Newton-Euler equations. The implementation of the sliding mode controller for the VTAV is described in Section 3. The simulation results are presented in Section 4. Section 5 concludes the paper.

2 Dynamic Model of the VTAV

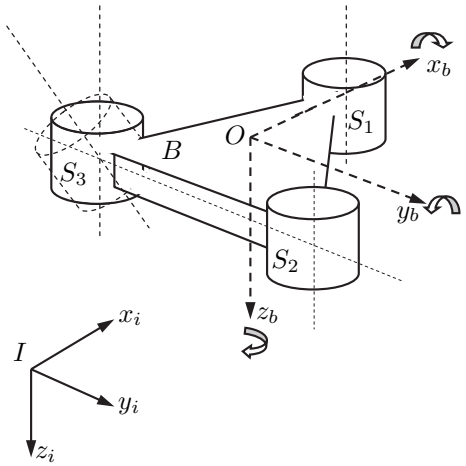

Figure 2: VTAV model and coordinate frames layout

The dynamic model of the VTAV were presented in [Yuan *et al.*, 2012] [Yuan and Katupitiya, 2013]. However, a brief description of the VTAV model is presented here for the clarity of the proposed controller. Contrary to the dynamic model presented in [Yuan

and Katupitiya, 2013] the model presented here considers the aerodynamic drag of the VTAV body as well in designing the controller.

The VTAV undergoes various types of forces and moments during flight. In order to analyse all these forces and moments with respect to a common coordinate system the following three coordinate systems are introduced.

The global coordinate frame, denoted by I contains the vector basis $[x_i\ y_i\ z_i]$. Coordinate frame B is attached to the VTAV body where the centre of gravity, O, is the origin of the vector basis $[x_b\ y_b\ z_b]$. Coordinate frame D with the vector basis $[x_d\ y_d\ z_d]$ is associated with each of the rear ducted fans of the VTAV. The orientations of the three coordinate frames are illustrated in Figure 2 and Figure 3. Rotational ma-

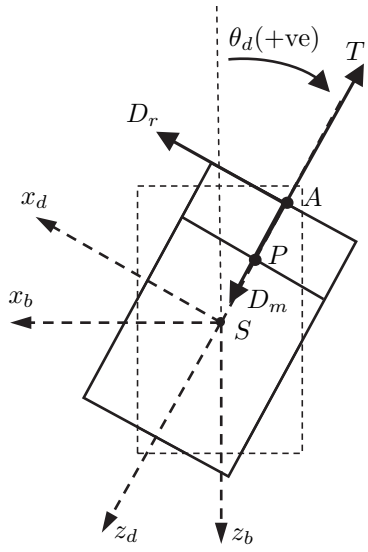

Figure 3: Ducted fan coordinate frame

trices R and R_d, based on Euler angles ϕ, θ and ψ, are introduced to transform the forces and moments from one frame to another. The Euler angles ϕ, θ and ψ represent VTAV's roll, pitch and yaw angles, respectively. The rotational matrix R represented by,

$$R = \begin{pmatrix} c_\Theta c_\Psi & s_\Theta s_\Phi c_\Psi - s_\Psi c_\Phi & s_\Theta c_\Phi c_\Psi + s_\Psi s_\Phi \\ c_\Theta s_\Psi & s_\Theta s_\Phi s_\Psi + c_\Psi c_\Phi & s_\Theta c_\Phi s_\Psi - c_\Psi s_\Phi \\ -s_\Theta & c_\Theta s_\Phi & c_\Theta c_\Phi \end{pmatrix}, \tag{1}$$

transforms forces and moments from coordinate frame B to I. Similarly the rotational matrix from B to D can be described as,

$$R_d = \begin{pmatrix} c_{\theta_d} & 0 & -s_{\theta_d} \\ 0 & 1 & 0 \\ s_{\theta_d} & 0 & c_{\theta_d} \end{pmatrix} \tag{2}$$

where θ_d is the vectoring angle as shown in Figure 3. Note that letters c and s represent *cosine* and *sine* functions, respectively.

As the VTAV is a rigid body, the Newton-Euler equations are used to derive the dynamic model of the vehicle represented by,

$$F_b = m\dot{v}_b + m(\omega_b \times v_b), \tag{3}$$

$$M_b = J_b\dot{\omega}_b + (\omega_b \times J_b\omega_b). \tag{4}$$

Here, m is the mass of the vehicle and $J_b = \text{diag}(I_{xx}, I_{yy}, I_{zz})$ is the moment of the inertia of the VTAV. The terms F_b and M_b denote the cumulative forces and moments acting on the VTAV with respect to the body fixed coordinate frame. The terms $v_b = \begin{bmatrix} v_{x_b} & v_{y_b} & v_{z_b} \end{bmatrix}^T$ and $\omega_b = \begin{bmatrix} \omega_{x_b} & \omega_{y_b} & \omega_{z_b} \end{bmatrix}^T$ represent the body linear and angular velocities, respectively.

2.1 Forces Acting on the VTAV

Gravity

The gravitational acceleration in global coordinate frame is, G_i=[0 0 g]^T. Therefore the gravitational force acting on the body coordinate frame can be denoted as,

$$G_b = mR^TG_i. \tag{5}$$

Thrust Force

The thrust generated by each of the ducted fans can be approximated as,

$$T = C_t\omega_f^2, \tag{6}$$

where C_t is the thrust coefficient and ω_f is the propeller angular speed. Therefore, the thrust force generated by a single ducted fan on the VTAV body can be derived as,

$$F_{Tb} = R_d^T \begin{bmatrix} 0 \\ 0 \\ -T \end{bmatrix}. \tag{7}$$

Ram Drag

Ram drag occurs due to the relative airflow with respect to the duct lip, mainly caused by sudden wind gusts and linear velocities of the UAV. Generally, the ram drag force acts perpendicular to the duct axis, z_d, and can be modeled as,

$$D = C_d\omega_f \begin{bmatrix} w_{x_d} \\ w_{y_d} \\ 0 \end{bmatrix} \tag{8}$$

Where, C_d is the drag coefficient of the duct. The terms w_{x_d} and w_{y_d} stand for the relative air velocities along x_d and y_d directions. Therefore, the ram drag force acting upon the body of the vehicle would be,

$$F_{Db} = R_d^T \begin{bmatrix} C_d\omega_f w_{x_d} \\ C_d\omega_f w_{y_d} \\ 0 \end{bmatrix} \tag{9}$$

Aerodynamic Drag

Aerodynamic drag occurs as a result of external forces such as wind gusts acting on the body of the vehicle. The aerodynamic drag force acting upon the VTAV body is modelled by the following equation,

$$F_{Ab} = C_a R^T \begin{bmatrix} w_{x_i} \\ w_{y_i} \\ w_{z_i} \end{bmatrix} \tag{10}$$

where $C_a = \text{diag}(A_{x_b}, A_{y_b}, A_{z_b})$ contains the aerodynamic drag coefficients of the vehicle along each axis and $[w_{x_i} w_{y_i} w_{z_i}]^T$ represent the relative air velocities in the global coordinate frame.

2.2 Moments acting on the VTAV

Gyroscopic Moments

The vectoring operation of the rear duct fans of the VTAV creates gyroscopic moments which affects the system adversely. The gyroscopic moment which occur due to the vectoring of a single ducted fan can be modeled as,

$$M_{Gb^v} = R_d^T I_d \omega_f \begin{bmatrix} -\omega_v \\ 0 \\ 0 \end{bmatrix} \tag{11}$$

where, ω_v is the vectoring angular rate and $I_d = \text{diag}(I_{x_d}, I_{y_d}, I_{z_d})$ is the inertia matrix of the propeller. Furthermore, the gyroscopic moments generated due to the pitch and roll movements of the entire vehicle body can be represented as,

$$M_{Gb} = R_d^T I_d \omega_f \begin{bmatrix} -\omega_{y_b} \\ -\omega_{x_b} \\ 0 \end{bmatrix} \tag{12}$$

where, ω_{y_b} and ω_{x_b} are the VTAV's pitch and roll angular rates, respectively. Note that the vehicle's yaw rate does not contribute to any gyroscopic moment.

Moments due to Thrust and Drag forces

Both the thrust and drag forces create moments around the vehicle centre of gravity, O. These moments can be represented as,

$$M_{Tb} = \overrightarrow{OP} \times F_{Tb}, \tag{13}$$

$$M_{Db} = \overrightarrow{OA} \times F_{Db}, \tag{14}$$

where P is the centre of the propeller plane and A is the centre of the duct lip plane as illustrated in Figure 3. Note that the aerodynamic drag forces act on the vehicle's center of gravity, hence does not create any moment on the body fixed frame.

The VTAV is made up of three ducted fans, with the ability to vector the rear two fans. Let subscripts 1, 2 and 3 represent the front, right and left ducted fans, respectively (see Figure 2). Utilizing the derived equations above, the total force and the moment acting on the VTAV body frame can be represented as,

$$F_b = \sum_{j=1}^{3} (F_{Tb_j} + F_{Db_j}) + G_b + F_{Ab}, \tag{15}$$

and,

$$M_b = \sum_{j=1}^{3} (M_{Tb_j} + M_{Db_j} + M_{Gb_j}) + \sum_{k=2}^{3} (M_{Gb_k^v}). \tag{16}$$

Substitution of (15) and (16) to (3) and (4) completes the nonlinear dynamic model of the VTAV [Yuan *et al.*, 2012][Yuan and Katupitiya, 2013].

3 Sliding Mode Controller Design

Consider the following dynamic system.

$$\dot{x}_1 = x_2 \tag{17}$$

$$\dot{x}_2 = f(x) + \Delta f(x) + d(x) + g(x)u \tag{18}$$

where, $f(x)$ is a nonlinear function, $\Delta f(x)$ an uncertain function and $d(x)$, an external disturbance. SMC methodology employs a discontinuous control law,u, which switches the control input between a couple of predefined control values such that the system under control reaches its desired states by sliding along a surface in state space represented by $S = 0$ which is also known as the sliding surface [Utkin, 1977][Khalil, 1996]. For a second order nonlinear dynamic system such as the VTAV, the general equation of the sliding surface can be represented as,

$$S = \lambda e + \dot{e}, \tag{19}$$

where λ is a positive constant and e represented by,

$$e = x - x_d, \tag{20}$$

is the error between the current state, x and the desired state, x_d. The control input u is designed such that the condition,

$$S\dot{S} < -\eta|S| \tag{21}$$

is satisfied. Here, η is a small positive constant. Therefore, based on the dynamic system stated in (17) and (18), the general equation for control input u takes the following form.

$$u = \frac{1}{g(x)}(-f(x) - \lambda\dot{e} - M\text{sign(S)}) \tag{22}$$

with $M > d_{max}(x) + \Delta f_{max}(x)$ and $g(x) \neq 0$

Based on Lyaponov stability criterium, the condition stated in (21) ensures $e \to 0$ asymptotically [Slotine and Li, 1991], converging the system states to their desired states.

However, the dynamic model of the VTAV is a MIMO nonlinear system, with control inputs coupled nonlinearly which makes it a difficult task to directly calculate the control inputs based on SMC methodology. Therefore, in order to implement the SMC methodology on the derived nonlinear model of the VTAV, the system model described by (3) and (4) are first combined to develop the following nonlinear dynamic system.

$$\dot{\mathbf{x}} = \mathbf{f}(\mathbf{x}) + \mathbf{\Delta f}(\mathbf{x}) + \mathbf{d}(\mathbf{x}) + \mathbf{g}(\mathbf{x})\mathrm{u} \tag{23}$$

where,

$$\dot{\mathbf{x}} = [\dot{v}_{x_b} \quad \dot{v}_{y_b} \quad \dot{v}_{z_b} \quad \dot{\omega}_{x_b} \quad \dot{\omega}_{y_b} \quad \dot{\omega}_{z_b}]^T \tag{24}$$

and using (15) and (16),

$$\mathbf{f}(\mathbf{x}) = \begin{bmatrix} -gs_\theta - (v_{z_b}\omega_{y_b} - v_{y_b}\omega_{z_b}) \\ gc_\theta s_\phi - (v_{x_b}\omega_{z_b} - v_{z_b}\omega_{x_b}) \\ gc_\theta c_\phi - (v_{y_b}\omega_{x_b} - v_{x_b}\omega_{y_b}) \\ ((I_{zz} - I_{yy})\omega_{y_b}\omega_{z_b})\frac{1}{I_{xx}} \\ ((I_{xx} - I_{zz})\omega_{x_b}\omega_{z_b})\frac{1}{I_{yy}} \\ ((I_{yy} - I_{xx})\omega_{x_b}\omega_{y_b})\frac{1}{I_{zz}} \end{bmatrix} \tag{25}$$

The vector $\mathbf{g}(\mathbf{x})$ can be represented by,

$$\mathbf{g}(\mathbf{x}) = \mathrm{diag}\left[\frac{1}{m}, 0, \frac{1}{m}, \frac{l}{I_{xx}}, \frac{e}{I_{yy}}, \frac{l}{I_{zz}}\right] \tag{26}$$

where parameters e and l stand for the linear distances from the centre of gravity to a ducted fan, along x_b and y_b axes, respectively.

The aerodynamic drag forces and their resulting moments are determined by the external wind disturbance at a given time. As the external wind disturbance cannot be measured, it is assumed that these forces and moments act as bounded disturbances on the system. Therefore, the disturbance vector $\mathbf{d}(\mathbf{x})$ can be derived as,

$$\mathbf{d}(\mathbf{x}) = \begin{bmatrix} F_{Ab_x} + \sum_{j=1}^{3} F_{Dbx_j} + d_1 \\ F_{Ab_y} + \sum_{j=1}^{3} F_{Dby_j} + d_2 \\ F_{Ab_z} + \sum_{j=1}^{3} F_{Dbz_j} + d_3 \\ \left(\sum_{j=1}^{3}(M_{Tbx_j} + M_{Dbx_j})\right)\frac{1}{I_{xx}} + d_4 \\ \left(\sum_{j=1}^{3}(M_{Tby_j} + M_{Dby_j})\right)\frac{1}{I_{yy}} + d_5 \\ \left(\sum_{j=1}^{3}(M_{Tbz_j} + M_{Dbz_j})\right)\frac{1}{I_{zz}} + d_6 \end{bmatrix} \tag{27}$$

where the values $d_j; j = 1 \ ... \ 6$ represent unmodelled external disturbances.

All model parametric uncertainties are lumped into the uncertainty vector $\mathbf{\Delta f}(\mathbf{x})$ and the resulting vector is presented as follows.

$$\mathbf{\Delta f}(\mathbf{x}) = [\Delta f_i(\mathbf{x})]^T; \quad i = 1 \ ... \ 6 \tag{28}$$

Vector $\mathbf{u}$ contains the control inputs to the VTAV system with,

$$\mathbf{u} = \begin{bmatrix} u_1 & u_2 & u_3 & u_4 & u_5 & u_6 \end{bmatrix}^T \tag{29}$$

where,

$$u_1 = -T_2 \sin\theta_{d2} - T_3 \sin\theta_{d3}, \tag{30}$$
$$u_2 = 0, \tag{31}$$
$$u_3 = -T_1 - T_2 \cos\theta_{d2} - T_3 \cos\theta_{d3}, \tag{32}$$
$$u_4 = -T_2 \cos\theta_{d2} + T_3 \cos\theta_{d3}, \tag{33}$$
$$u_5 = 2T_1 - T_2 \cos\theta_{d2} - T_3 \cos\theta_{d3} \tag{34}$$
$$u_6 = T_2 \sin\theta_{d2} - T_3 \sin\theta_{d3} \tag{35}$$

Here, the terms T_1, T_2 and T_3 represent the thrust values of the three fans, and θ_{d2}, θ_{d3} denote the vectoring angles of the VTAV.

The variable structure control law is then derived for each subsystem using the control input vector $\mathbf{u}$, ensuring that the system reaches its desired states from any given initial condition of the VTAV. The introduction of vector $\mathbf{u}$ virtually uncouples all the dynamic equations simplifying the implementation of the sliding mode controller.

For this particular system, five separate sliding surfaces will be introduced. A given sliding surface, S_i for a particular state takes the general form defined by (19). The following assumptions are made prior to the implementation of SMC.

- All states can be directly measured or estimated using an observer.
- All external disturbances and parametric uncertainties are bounded in the following manner.

$$|\mathbf{d}(\mathbf{x})| \leq \mathbf{d_{max}} \tag{36}$$
$$\mathbf{d_{max}} = [d_{1_{max}} \quad d_{2_{max}} \quad ... \quad d_{6_{max}}]^T \tag{37}$$
$$|\mathbf{\Delta f}(\mathbf{x})| \leq \mathbf{\Delta f_{max}} \tag{38}$$
$$\mathbf{\Delta f_{max}} = [\Delta f_{1_{max}} \quad ... \quad \Delta f_{6_{max}}]^T \tag{39}$$

3.1 Attitude Control

The main aim of the controller is to operate the VTAV with minimum roll and pitch movements. The stepwise approach to maintain this requirement is described from Section 3.1 onwards.

Yaw Control

For operations such as terrain mapping it is desirable for the VTAV to maintain zero roll and pitch angles. Furthermore, the VTAV is under actuated in the y_b direction. As such, to reach a point in the y_i direction the VTAV first needs to go through a yaw motion and then translate in the x_b direction. Therefore, the desired yaw angle for a given setpoint can be derived as,

$$\psi_d = \tan^{-1}\left(\frac{x_{y_{id}}}{x_{x_{id}}}\right) \tag{40}$$

where, $x_{x_{id}}$ and $x_{y_{id}}$ are the desired global x and y set points, respectively. Once the system reaches ψ_d, the position set point lies on the vehicles body (x_b, z_b) plane. This way the need to translate in the under-actuated y_b direction is eliminated. Based on SMC methodology, in order to reach ψ_d the control input u_6 is derived as,

$$u_6 = u_{6eq} + u_{6disc}, \tag{41}$$

where the subscripts eq and $disc$ identifies the equivalent and discontinuous components of the SMC control effort. The two components are given by,

$$\begin{aligned} u_{6eq} &= [(-\omega_{z_b} + \omega_{z_{bd}})I_{zz} \\ &\quad -(I_{yy} - I_{xx})\omega_{x_b}\omega_{y_b}]/l \qquad (42) \\ u_{6disc} &= -M_6 \text{ sign}(S_6)/l \qquad (43) \end{aligned}$$

where $S_6 = 0$ is the corresponding sliding surface for the yaw dynamics. $S_6 = 0$ takes the general sliding surface form represented by (19) with $\lambda = 1$. In order to satisfy (21) which ensures convergence of the system, the switching gain M_6 is selected such that,

$$M_6 > d_{6_{max}} + \Delta f_{6_{max}} \tag{44}$$

Hence, the amount of disturbance and uncertainties the controller can withstand depends on the maximum available control resources of the system.

Pitch Control

As the aim of the controller is to maintain minimum roll and pitch movements, the VTAV pitch angle θ should be maintained at $\theta_d = 0$ for all $t > 0$. The pitch control input,

$$u_5 = u_{5eq} + u_{5disc}, \tag{45}$$

where,

$$\begin{aligned} u_{5eq} &= [(-\omega_{y_b} + \omega_{y_{bd}})I_{yy} \\ &\quad -(I_{xx} - I_{zz})\omega_{x_b}\omega_{z_b}]/e \qquad (46) \\ u_{5disc} &= -M_5 \text{ sign}(S_5)/e \qquad (47) \end{aligned}$$

with the switching gain M_5 satisfying

$$M_5 > d_{5_{max}} + \Delta f_{5_{max}} \tag{48}$$

ensures the pitch angle of the VTAV is maintained at 0 at all times.

Roll Control

As mentioned earlier it is desirable to maintain the roll angle of the VTAV at $\phi = 0$ for $t > 0$. While lateral wind gusts can force the VTAV off course, in the absence of such disturbances the roll angle must be maintained at zero. If there were to be such disturbances, a non-zero transient roll angle will result through the lateral off set correction control.

In order to solve this issue the desired roll angle ϕ_d is defined as,

$$\phi_d = \rho e_i + \dot{e}_i \tag{49}$$

with,

$$e_i = x_{y_i} - \tan(\psi_d)x_{x_i} \tag{50}$$

where x_{x_i} and x_{y_i} are measured distances along global x_i and y_i directions, respectively. ρ is a positive constant. As a result $e_i = 0$ when the VTAV heading is in the correct direction. Consequently, when the vehicle drifts laterally due to winds in y_b direction, the value of e_i becomes non-zero, resulting in $\phi_d \neq 0$. The result obtained for ϕ_d is then applied to the general sliding surface for roll angle in the following manner.

$$S_4 = \lambda_4[\phi - (-\phi_d)] + [\omega_{bx} - \omega_{bx_d}] \tag{51}$$

To summarize, the desired roll angle is 0 when undesired translations in y_b direction is zero. Whenever there is a sudden lateral wind gust the desired roll angle becomes non-zero as shown in (49). Therefore, the final control input for roll dynamics would be,

$$\begin{aligned} u_4 &= u_{4eq} + u_{4disc} \qquad (52) \\ u_{4eq} &= [(-\omega_{bx} - \dot{\phi}_d)I_{yy} - \\ &\quad (I_{zz} - I_{yy})\omega_{by}\omega_{bz}]/l \qquad (53) \\ u_{4disc} &= -M_4 \text{ sign}(S_4)/l \qquad (54) \end{aligned}$$

with,

$$M_4 > d_{4_{max}} + \Delta f_{4_{max}} \tag{55}$$

3.2 Position Control

The nonlinear dynamic equations of the VTAV is derived with respect to the vehicle body coordinate system. Therefore, the desired position setpoints need to be transformed to the VTAV body coordinate system as well.

$$\begin{bmatrix} x_{x_{bd}} \\ x_{y_{bd}} \\ x_{z_{bd}} \end{bmatrix} = R^T \begin{bmatrix} x_{x_{id}} \\ x_{y_{id}} \\ x_{z_{id}} \end{bmatrix}, \tag{56}$$

where, $[x_{x_{id}}, x_{y_{id}}, x_{z_{id}}]$ is the desired global position coordinate which the vehicle need to reach in finite time. Control inputs u_1 and u_3 are responsible for tracking $x_{x_{id}}$ and $x_{z_{id}}$, respectively. Implementation of SMC methodology on the 1st and 3rd rows of the dynamic system stated in (23) yields,

$$\begin{aligned} u_1 &= u_{1eq} + u_{1disc} \qquad (57) \\ u_{1eq} &= [(-v_{x_b} + v_{x_{bd}}) + gs_\theta \\ &\quad +(v_{z_b}\omega_{y_b} - v_{y_b}\omega_{z_b})]m \qquad (58) \\ u_{1disc} &= -M_1 m \text{ sign}(S_1), \qquad (59) \end{aligned}$$

and

$$\begin{aligned} u_3 &= u_{3eq} + u_{3disc} \qquad (60) \\ u_{3eq} &= [(-v_{z_b} + v_{z_{bd}}) - g\cos\theta\cos\phi \\ &\quad +(v_{y_b}\omega_{x_b} - v_{x_b}\omega_{y_b})]m \qquad (61) \\ u_{3disc} &= -M_3 m \text{ sign}(S_3), \qquad (62) \end{aligned}$$

where, for reasons similar to those derived for (44),

$$M_1 > d_{1_{max}} + \Delta f_{1_{max}} \quad (63)$$
$$M_3 > d_{3_{max}} + \Delta f_{3_{max}} \quad (64)$$

The vehicle is under actuated in y_b direction. However, the limitations caused by the under actuation was reduced by the yaw control mechanism implemented in Section 3.1. The yaw control derived in (40) makes sure that the final desired position of the VTAV always lies on the vehicle $x_b - z_b$ plane. Furthermore, the controlled roll movement derived in (52) compensates for any disturbances along y_b direction ensuring that the VTAV maintains its desired path.

After obtaining the virtual control inputs, the next step is to derive the actual control inputs to the system. The actual control input to the system consists of three thrust inputs (T_1, T_2, T_3) and two vectoring inputs $(\theta_{d2}, \theta_{d3})$. Solving the nonlinear equation set (30)-(35) returns the actual control inputs to be applied to the VTAV. Hence, the final controls for the thrusts and vectoring angles are,

$$T_1 = \frac{\mathrm{u}_1 - \mathrm{u}_3}{3} \quad (65)$$
$$T_2 = 0.5\sqrt{(\mathrm{u}_6 - \mathrm{u}_1)^2 + \left(\frac{-\mathrm{u}_5 - 2\mathrm{u}_3 - 3\mathrm{u}_4}{3}\right)^2} \quad (66)$$
$$T_3 = 0.5\sqrt{(\mathrm{u}_6 + \mathrm{u}_1)^2 + \left(\frac{-\mathrm{u}_5 - 2\mathrm{u}_3 + 3\mathrm{u}_4}{3}\right)^2} \quad (67)$$
$$\theta_{d2} = \tan^{-1}\left(\frac{3(\mathrm{u}_1 - \mathrm{u}_6)}{\mathrm{u}_5 + 2\mathrm{u}_3 + 3\mathrm{u}_4}\right) \quad (68)$$
$$\theta_{d3} = \tan^{-1}\left(\frac{3(\mathrm{u}_1 + \mathrm{u}_6)}{\mathrm{u}_5 + 2\mathrm{u}_3 - 3\mathrm{u}_4}\right) \quad (69)$$

The corresponding propeller speed can be calculated through (6).

3.3 Actuator Dynamics and Chattering

The VTAV has three brushless DC motors to drive the fans and two servo motors for vectoring the thrusters. The dynamics of these actuators needs to be taken into consideration when developing a practically applicable controller. The actuator dynamics can be approximated as,

$$G_{act_i} = \frac{\alpha_i}{\tau_i s + 1} \quad (70)$$

where, α_i and τ_i represent the gain and time constant of the i^{th} actuator. The control inputs derived in Section 3 could excite these actuator dynamics and induce chattering [Young *et al.*, 1999][Utkin *et al.*, 2009], owing to the high frequency discontinuous switching of the control inputs. In order to eliminate chattering, the sign(S) term is replaced with a saturation function, sat(S). The sat(S) function confines the system to a boundary layer around the sliding surface, while eliminating the undesired chattering effect. The sat(S) function is defined as,

$$\mathrm{sat}(S) = \begin{cases} S/\beta & for \quad |S| < \beta \\ \mathrm{sign}(S) & for \quad |S| \geq \beta \end{cases} \quad (71)$$

where β is the width of the boundary layer.

4 Simulation Results

Simulations were carried out to verify the performance of the proposed sliding mode controller. As the designed controller will be implemented in a digital system, the discretization effect introduced by such systems was also taken into consideration, with a sampling time of 10 ms. Actuator dynamics introduced in Section 3.3 were also included in the final dynamic model. Two test cases under different conditions were chosen to investigate the performance of the controller.

VTAV parameters used for the simulations are shown in Table 1.

Table 1: Nominal Values of VTAV Parameters

Parameter(unit)	Value	Parameter(unit)	Value
m (kg)	2.0	d (m)	0.231
g (ms^{-2})	9.81	e (m)	0.1155
I_d (kgm^2)	5.0×10^{-5}	f (m)	0.2
I_{xx} (kgm^2)	0.0229	$\alpha_1 = \alpha_2 = \alpha_3$	41.2
I_{yy} (kgm^2)	0.1279	$\alpha_4 = \alpha_5$	1
I_{zz} (kgm^2)	0.0917	$\tau_1 = \tau_2 = \tau_3$	0.03
C_d	5×10^{-4}	$\tau_4 = \tau_5$	0.02
C_t	1.8×10^{-4}	$A_{xb} = A_{yb} = A_{zb}$	2.0×10^{-5}

4.1 Test 1: Attitude test

One of the main advantages of a nonlinear control methodology over its linear counterpart is its ability to handle a system over a wide range of operating points. In order to test this condition the initial attitude of the VTAV was set to $\Phi = \theta = \Psi = 57.3°$. The aim of the controller is to bring the VTAV to its zero attitude position in the presence of external wind disturbances and parametric uncertainties, whilst maintaining the vehicle's global position stationary as well. For this test, an external wind vector of $W_i = [3 \quad 0 \quad 2]^T m/s$ was introduced to the simulation coming into effect at $t = 0s$. It is also assumed that the measured inertia values have a maximum error of 10% with respect to the actual values.

The results are presented in Figure 4 and Figure 5. The VTAV attitude is corrected in finite time in the presence of external wind disturbances and parametric uncertainties as shown in Figure 4. The global position also returns good results as shown in Figure 5 with a maximum error of 3 cm in z_i direction due to the saturation function introduced. If sat(S) is replaced with sign(S) the error disappears albeit with undesirable chattering.

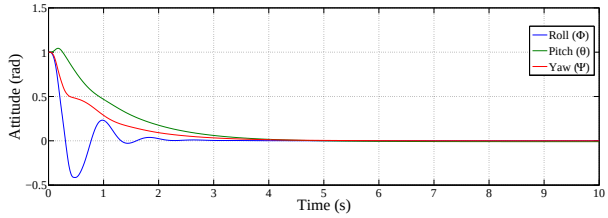

Figure 4: Test1: Attitude of VTAV

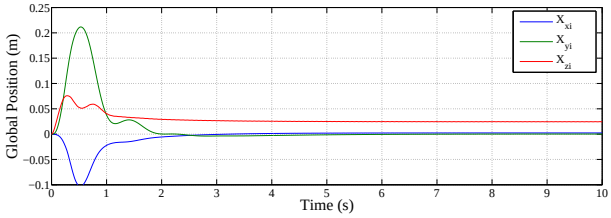

Figure 5: Test1: Global position of VTAV

4.2 Test 2: Position test

The ability of the controller to track down a given set-point in the presence of wind disturbances and parametric uncertainties was evaluated next. The external disturbances and parametric uncertainties applied to the system are as follows.

- A continuous wind of magnitude 3 m/s along x_i.
- A continuous wind of magnitude 2 m/s along y_i.
- The wind gust along y_i increases by 1 m/s during the time duration of $t = 9$ sec. to $t = 11$ sec.
- The parametric uncertainty of I_{xx}, I_{yy}, I_{zz} and C_d are represented by a 10% variation of their values.

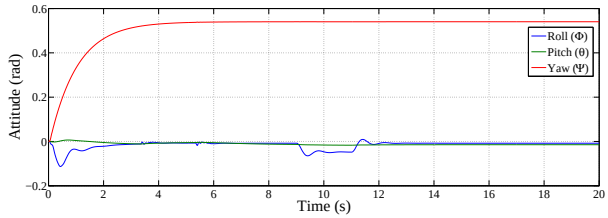

Figure 6: Test2: Attitude of VTAV

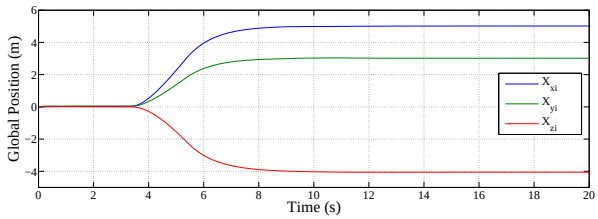

Figure 7: Test2: Global position of VTAV

The desired position was provided as $x_{id} = [5 \quad 3 \quad -4]^T$. Results show that the system performs well under these conditions. In order to track the desired global y_i coordinate, $x_{y_{id}}$, the VTAV goes through a yaw motion from $t = 0s$ to $t = 3.38s$ as defined by (40). Due to the relative air velocity in y_b direction, the vehicle creates a matching roll motion as defined by (49). It is important to note that the roll motion occurs *only* when a relative air velocity in the y_b direction exists. The roll motion adjusts again as illustrated in Figure 6, when the wind velocity increases during $t = 9s$ to $t = 11s$. As a result the VTAV maintains its stability and tracks the trajectory with accuracy as presented in Figure 7.

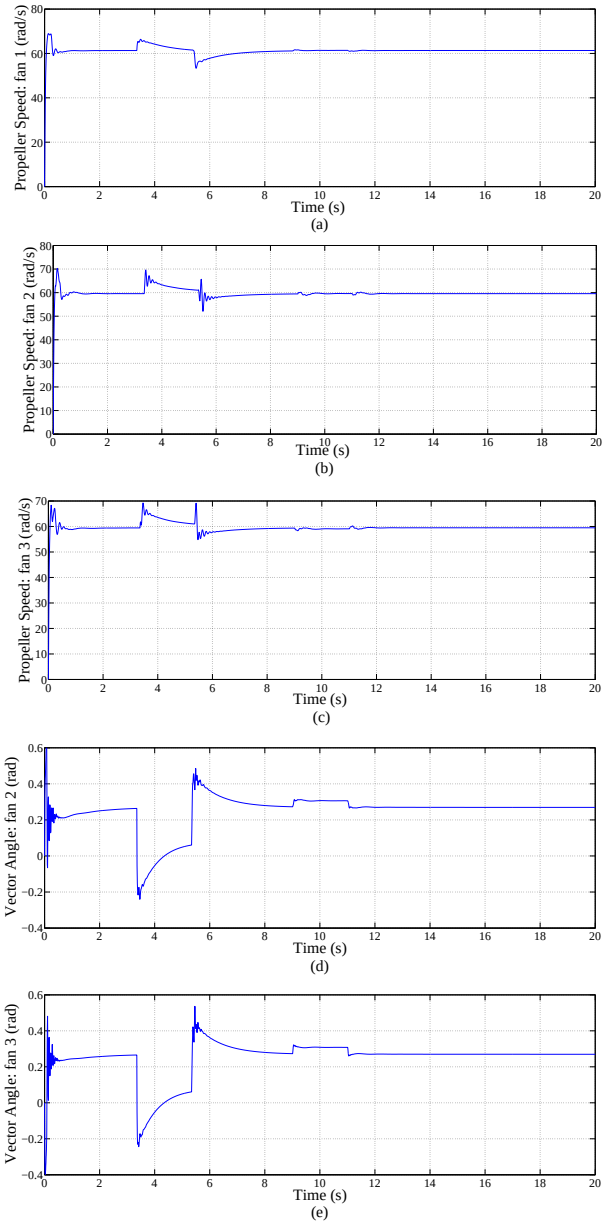

Figure 8: Propeller speeds and vector angles of VTAV for Test: 2

The corresponding propeller speeds and vectoring angles are shown in Figure 8. Note that the vectoring angles $\theta_{d2}, \theta_{d2} \neq 0$ at the end of the simulation in

order to keep the vehicle stationary in the presence of external disturbances. The small oscillations which exist for a short duration on Fig. 8 at $t = 3.38s$ and $t = 5.7s$ are due to the gyroscopic moments of the VTAV. However, the controller successfully compensates the effects of such factors whilst maintaining the stability of the system.

5 Conclusions

The paper presented the control of a vectored thrust aerial vehicle that is designed for special purposes such as terrain mapping which will significantly benefit from the ability to fly with zero roll and pitch. Such an arrangement will enable the sensors to be reliably directed at the desired terrain patch. Given that the system is nonlinear and that there is the possibility of parametric uncertainties and the presence of disturbances, sliding mode control design approach was chosen to develop robust controllers. The designed controllers were tested under different test conditions and it was demonstrated that the controllers operated well. The results further suggest that the controllers performs well even with digital implementation provided that the control parameters are tuned properly.

References

[Bertrand *et al.*, 2011] Sylvain Bertrand, Nicolas Guénard, Tarek Hamel, Hélène Piet-Lahanier, and Laurent Eck. A hierarchical controller for miniature VTOL UAVs: Design and stability analysis using singular perturbation theory. *Control Engineering Practice*, 19(10):1099–1108, October 2011.

[Derafa *et al.*, 2012] L. Derafa, a. Benallegue, and L. Fridman. Super twisting control algorithm for the attitude tracking of a four rotors UAV. *Journal of the Franklin Institute*, 349(2):685–699, March 2012.

[Guruganesh *et al.*, 2012] R Guruganesh, B. Bandyopadhyay, and Hemendra Arya. Robust stabilization of Micro Aerial Vehicle using sliding mode control. In *12th International Workshop on Variable Structure Systems*, pages 397–403, Mumbai, January 2012. Ieee.

[Hess and Bakhtiari-Nejad, 2008] Ronald a. Hess and Maryam Bakhtiari-Nejad. Sliding-Mode Control Applied of a Nonlinear Model of an Unmanned Aerial Vehicle. *Journal of Guidance, Control, and Dynamics*, 31(4):1163–1166, July 2008.

[Hess and Wells, 2003] R.A. Hess and S.R. Wells. Sliding Mode Control Applied to Reconfigurable Flight Control Design. *Journal of Guidance, Control, and Dynamics*, 26(3):452–462, 2003.

[Johnson and Turbe, 2006] Eric N Johnson and Michael A Turbe. Modeling, Control, and Flight Testing of a Small Ducted-Fan Aircraft. *Journal of Guidance, Control, and Dynamics*, 29(4), 2006.

[Khalil, 1996] Hassan K Khalil. *Nonlinear Systems*. Prentice Hall, NJ, second edi edition, 1996.

[Khelfi and Kacimi, 2012] Mohamed Faycal Khelfi and Abderrahmane Kacimi. Robust control with sliding mode for a quadrotor unmanned aerial vehicle. In *IEEE International Symposium on Industrial Electronics*, pages 886–892. Ieee, May 2012.

[Kumon *et al.*, 2010] Makoto Kumon, Hugh Cover, and Jayantha Katupitiya. Hovering control of vectored thrust aerial vehicles. In *IEEE International Conference on Robotics and Automation*, pages 1149–1154, Alaska,USA, May 2010. Ieee.

[Naldi *et al.*, 2008] R. Naldi, L. Marconi, and A. Sala. Modelling and control of a miniature ducted-fan in fast forward flight. In *2008 American Control Conference*, pages 2552–2557, Washington, USA, June 2008. Ieee.

[Naldi *et al.*, 2010] Roberto Naldi, Luca Gentili, Lorenzo Marconi, and Andrea Sala. Design and experimental validation of a nonlinear control law for a ducted-fan miniature aerial vehicle. *Control Engineering Practice*, 18(7):747–760, July 2010.

[Pflimlin *et al.*, 2010] J.-M. Pflimlin, P. Binetti, P. Souères, T. Hamel, and D. Trouchet. Modeling and attitude control analysis of a ducted-fan micro aerial vehicle. *Control Engineering Practice*, 18(3):209–218, March 2010.

[Slotine and Li, 1991] J.J.E. Slotine and W. Li. *Applied nonlinear control*. Prentice Hall, 1 edition, 1991.

[Utkin *et al.*, 2009] Vadim I Utkin, J. Guldner, and J. Shi. The Chattering Problem. In *Sliding Mode Control in Electro-Mechanical Systems*, chapter 8, pages 159–204. Second edition, 2009.

[Utkin, 1977] Vadim I Utkin. Variable Structure Systems with Sliding Modes. *IEEE transactions on Automatic Control*, AC-22(2):212–222, 1977.

[Wang *et al.*, 2007] H Wang, Daobo Wang, Xinwen Niu, and H Duan. Modeling and hover control of a novel unmanned coaxial rotor/ducted-fan helicopter. In *International Conference on Automation and Logistics*, number 2006, pages 1768–1773, Jihan, China, 2007.

[Young *et al.*, 1999] K.D. Young, V.I. Utkin, and U. Ozguner. A control engineer's guide to sliding mode control. *IEEE Transactions on Control Systems Technology*, 7(3):328–342, May 1999.

[Yu *et al.*, 2010] Yali Yu, Changhong Jiang, and Haiwei Wu. Backstepping control of each channel for a quadrotor aerial robot. In *2010 International Conference on Computer, Mechatronics, Control and*

Electronic Engineering, pages 403–407. Ieee, August 2010.

[Yuan and Katupitiya, 2013] Wei Yuan and Jay Katupitiya. Dynamic Modelling and Control of a Vectored Thrust Aerial Vehicle. In *IEEE/ASME International Conference on Advanced Intelligent Mechatronics*, pages 1361–1366, Wollongong, Australia, 2013.

[Yuan *et al.*, 2012] Wei Yuan, Hiranya Jayakody, and Jay Katupitiya. Dynamic Modelling and Analysis of a Vectored Thrust Aerial Vehicle. In *Australasian Conference onRobotics and Automation-ACRA*, pages 3–5, Wellington, New Zealand, 2012. ARAA.

[Zhang *et al.*, 2010] Chao Zhang, Zi Yang Zhen, Dao Bo Wang, and Xin Yu Meng. Optimal Control for Thrust Vectoring Unmanned Aerial Vehicle. *Key Engineering Materials*, 439-440:292–297, June 2010.